Global Change Biology

Global Change Biology (2010) **16**, 546–560, doi: 10.1111/j.1365-2486.2009.02037.x

Impact of insect defoliation on forest carbon balance as assessed with a canopy assimilation model

KARINA V. R. SCHÄFER*, KENNETH L. CLARK†, NICHOLAS SKOWRONSKI†‡ and ERIK P. HAMERLYNCK§

*Department of Biological Sciences, Rutgers University, 195 University Ave., Newark, NJ 07102, USA, †Silas Little Experimental Forest, USDA Forest Service, 501 Four Mile Rd, New Lisbon, NJ 08064, USA, ‡Department of Ecology, Evolution and Natural Resources, Graduate Program in Ecology and Evolution, Rutgers University, 14 College Farm Road, New Brunswick, NJ 08901-8551, USA, §USDA-ARS Southwest Watershed Research Center, Arizona, 2000 E. Allen Road, Tucson, AZ 85719, USA

Abstract

Disturbances such as fire, hurricanes, and herbivory often result in the net release of CO_2 from forests to the atmosphere, but the magnitude of carbon (C) loss is poorly quantified and difficult to predict. Here, we investigate the carbon balance of an oak/pine forest in the New Jersey Pine Barrens using the Canopy Conductance Constrained Carbon Assimilation (4C-A) model. The 4C-A model utilizes whole-tree sap-flux and leaf-level photosynthetic gas exchange measurements at distinct canopy levels to estimate canopy assimilation. After model parameterization, sensitivity analyses, and evaluation against eddy flux measurements made in 2006, the model was used to predict C assimilation for an undisturbed year in 2005, and in 2007 when the stand was completely defoliated for 2–3 weeks during an infestation of gypsy moths (*Lymantria dispar* L.). Following defoliation, only 50% of the foliage reemerged in a second flush. In 2007, canopy net assimilation (A_{nC}), as modeled with the 4C-A, was reduced to approximately 75% of A_{nC} in 2006 (940 vs. 1240 g C m^{-2} a^{-1}). Overall, net primary production (NPP) in 2007 was approximately 240 g C m^{-2} a^{-1} (vs. 250 g C m^{-2} a^{-1} in 2006), with 60% of NPP allocated to foliage production, a short-term carbon pool. Woody biomass accumulation, a long-term carbon pool, was reduced by 20% compared with the previous year (72 vs. 57 g C m^{-2} a^{-1} in 2006 and 2007, respectively). The overall impact of the defoliation spanned 21% of upland forests (320 km^2) in the New Jersey Pine Barrens, representing a significant amount of overall C not being taken up from the atmosphere by the forest, thus not accumulated in the biosphere.

Keywords: 4C-A, canopy assimilation, defoliation, New Jersey Pine Barrens, sap flux

Received 18 February 2009; revised version received 15 June 2009 and accepted 6 July 2009

Introduction

In an effort to mitigate CO_2 emissions to the atmosphere, there is increasing interest in quantifying and predicting carbon (C) dynamics and long-term C storage in forests (CCSP, 2007). Recent research has demonstrated that rates of C uptake and storage are not only a function of climatic and edaphic factors, but also of site land-use history (Roxburgh *et al*., 2007; Gough *et al*., 2008; Scheller *et al*., 2008) as well as disturbances such as ice storms (McCarthy *et al*., 2006), hurricanes (McNulty, 2002; Chambers *et al*., 2007), fire (Ryan, 2002; Gough *et al*., 2007; Vargas *et al*., 2008), and herbivory (Gromtsev, 2002; Eisenbies *et al*., 2007; Fajvan *et al*., 2008; Kurz *et al*., 2008; Running, 2008; Clark *et al*., 2009). Disturbance events directly affect C uptake through loss of leaves and needles, and indirectly by altering detrital pools, nutrient dynamics, and nutrient availability, which in turn can affect leaf biochemical function. An increase in temperature and changes in precipitation regimes are expected with global climate change. Hurricanes and droughts, which increase tree falls and forest fires, may also increase in the future (Dale *et al*., 2001; IPCC, 2007). In temperate regions, higher temperatures are also likely to increase the frequency and severity of insect outbreaks (Jönsson *et al*., 2008). Epidemic insect outbreaks have been recently shown to reduce C uptake by forests significantly (Kurz *et al*., 2008), and will affect long-term C storage.

Indirect effects of disturbance, such as an acceleration of microbial activity and fungal decay following increased

Correspondence: Karina V. R. Schäfer, tel. +1 973 353 1008, fax +1 973 353 5518, e-mail: karinavr@andromeda.rutgers.edu

detrital inputs, can lead to altered patterns of nutrient cycling. Fungal decay in living woody stems further enhances windfall and mortality during windy conditions (Matlack *et al*., 1993). With increased disturbance in forest ecosystems, additional carbon will be transferred into detrital pools on the forest floor and in soil (McCarthy *et al*., 2006). Climate change may further impact carbon and nutrient dynamics by extending the growing season of some species, which alters competitive interactions and recruitment in the long term following disturbances (Matlack *et al*., 1993; Little, 1998; Sitch *et al*., 2008).

Mathematical models provide a way to examine the nonlinear and complex nature of biophysical interactions that govern biosphere-atmosphere exchanges in forest systems that make straightforward assessments difficult. For example, while CO_2 flux measurements can track changes in ecosystem function across sites and over seasons, they cannot directly assess the relative contributions of biotic and abiotic factors regulating whole-forest C-balance. These mechanisms, however, can be assessed via modeling approaches. Initial results from some large-scale forest C-cycle models such as BIOME BGC (Thornton *et al*., 2002), PNET-CN (Pan *et al*., 2006) or 3-PG (Landsberg & Waring, 1997) have demonstrated that these models are poor at predicting some disturbance impacts, because they typically calculate canopy conductance based on meteorological variables, and are not able to incorporate concurrent changes in canopy structure, leaf area, and leaf-level physiological activity during and following disturbance events (Wang & Jarvis, 1990; Collatz *et al*., 1991; Leuning, 1995; Baldocchi & Meyers, 1998). Simulating the concomitant drop in water flux associated with loss of foliage is difficult when models are driven solely using meteorological variables. Modeling conductance can be especially difficult in nutrient-poor and water-limited forests, which may require soil moisture corrections (Lai *et al*., 2000; Pan *et al*., 2006). In addition, the remotely sensed data that is often used to parameterize these models may lack the spatial and temporal resolution needed to capture the dynamics of foliage display associated with disturbance effects.

Canopy assimilation models enable the assessment of C uptake and the factors behind overall uptake strength in forested stands (Schulze, 2006), including changes in leaf area (McCarthy *et al*., 2007), nutrient limitations [via reduction in carboxylation efficiency (CE)], and altered canopy conductance (Schulze, 2006). In order to assess canopy C uptake accurately during and following disturbance events, carbon assimilation models such as the Canopy Conductance Constrained Carbon Assimilation model (4C-A, Schäfer *et al*., 2003; Kim *et al*., 2008) must detect the temporal intensity of the disturbance allowing for the estimation of C dynamics before, during, and after these events. One of the advantages of the 4C-A model is that direct measurements of canopy conductance (G_C) are used, avoiding problems of modeling G_C during and following a disturbance. Direct leaf-area dynamics can also be accounted for by modeling the light regime at different canopy levels.

In this study, we used the 4C-A model to predict canopy C balance of an upland oak/pine forest in the New Jersey Pine Barrens, a nutrient-poor and water-limited environment (Dighton *et al*., 2004; Pan *et al*., 2006). The 4C-A model was first parameterized using field data collected in 2006. Model sensitivity to (a) G_C, (b) CE, (c) leaf-area distribution (using a Gaussian leaf-area profile that closely resembled the measured leaf-area density profile measured via LiDAR), and (d) prolonged growing season (i.e. leaf on condition prolonged by 1 week at onset and 1 week at senescence) was assessed. Model results for 2006 were then compared with eddy flux measurements and forest census measurements. Following sensitivity analysis and evaluation, the 4-CA model was applied to 2005, a disturbance-free year, and to 2007, when gypsy moth completely defoliated the canopy and understory for approximately 3 weeks. A second flush of foliage then produced approximately 50% of the foliage in previous growing seasons in 2005 and 2006.

Materials and methods

After a brief description of the site and the 4C-A model (details of the model can be found in Schäfer *et al*., 2003), the measurements required for estimating model parameters are described, followed by an outline of the sensitivity analyses performed using data from 2006. Next described is the evaluation of model predictions against eddy flux and biometric measurements. Finally, we use the 4C-A model to assess C dynamics in 2005, a disturbance-free year and 2007, a defoliation year.

Study Site

This study was conducted at the Rutgers University Pinelands Research Station, also known as the USDA Forest Service's Silas Little Experimental Forest, located in Pemberton Township in the Pine Barrens of southern New Jersey, USA (N39°55′0″, W74°36′0″). Mean annual temperature is 11.5 °C, with an annual precipitation of 1123 (± 182) mm, with 2400 total annual hours of sunshine. The soil is characterized as a podzol, underlain by late Miocene fluvial sediments of the Kirkwood formation, and overlain with Cohansey sandy soil (Rhodehamel, 1998), with low nutrient content and

Published 2009

Table 1 Forest stand characteristics of the Rutgers Pineland Research Station in 2006.

Attribute	Silas Little	Subplot
Stem density (stems ha^{-1})		
Pine	90 ± 19	122
Oak	1233 ± 293	1216
Total	1323 ± 300	1342
Basal area ($m^2 ha^{-1}$)		
Pine	4.4 ± 2.4	1.3
Oak	11.5 ± 1.4	14.9
Total	15.9 ± 2.5	16.2
Height (m)		
Pine	11.2 ± 2.9	5.1 ± 4.6
Oak	9.3 ± 1.0	8.7 ± 4.8
Total	9.5 ± 1.0	8.4 ± 4.9
Canopy aboveground biomass ($g m^{-2}$)		
Pine	2134 ± 1179	518
Oak	6360 ± 736	6925
Total	8494 ± 1220	7443
Canopy belowground biomass ($g m^{-2}$)		
Pine		140
Oak		3962
Total		4101
Understory biomass ($g m^{-2}$)		
Shrub	168 ± 38	
Oak	20 ± 15	
Total	189 ± 35	
Forest floor mass ($g m^{-2}$)		
Fine litter	845 ± 45	
Wood	223 ± 47	
Total	1068 ± 75	

Silas Little data are from five 201 m^2 plots located within 100 m of the flux tower (Clark *et al.*, 2009), and the subplot is a 0.3 ha pie slice northwest of the flux tower that contains the sap-flux measurements.
Values are means ± 1 SE.
Canopy biomass was calculated using allometric relationships from Whittaker & Woodwell (1968).

cation exchange capacity (Markley, 1998). The study area is relatively flat with a mean elevation of 33 m. The dominant tree species are *Quercus prinus* Willd. (chestnut oak), *Quercus velutina* Lam. (black oak), and *Quercus coccinia* Münchh. (scarlet oak), with scattered *Pinus rigida* Mill. (pitch pine), and *Pinus echinata* Mill. (shortleaf pine). Less abundant oaks at the site include *Quercus stellata* Wangenh. (post oak), and *Quercus alba* L. (white oak) (Table 1, see also Skowronski *et al.*, 2007; Clark *et al.*, 2009). The canopy leaf area index (LAI) derived from litterfall was 3.6 in 2006. The understory was comprised of *Gaylussaccia baccata* (Wangenh.), K. Koch (black huckleberry), and *Vaccinium* spp., with a LAI of 0.45 $m^2 m^{-2}$ in 2006, derived from clip plots (n = 10–20 of 1.0 m^2).

Modeling approach

The Canopy Conductance Constrained Carbon Assimilation model (4C-A) uses sap-flux-derived estimates of G_C to constrain net assimilation modeled throughout the canopy by a leaf-level hybrid approach defined by Katul *et al.* (2000). This approach approximates the nonlinear Farquhar model (Farquhar *et al.*, 1980) for net assimilation (A_{net}) to internal CO_2 concentration (C_i) with a linear relationship, and then C_i is set to a constant after a critical conductance value is reached. Light regimes for sunlit and shaded leaves are modeled using algorithms developed by DePury & Farquhar (1997) and Campbell & Norman (1998) at each 1 m height level throughout the canopy. Modeled light regimes are used to calculate leaf-level conductance to water vapor (g_W), with light-g_W response functions derived from gas exchange measurements. Leaf area weighted g_w in each canopy level is then constrained to match G_C derived from sap-flux measurements (for a detailed description of 4C-A see Schäfer *et al.*, 2003). Conductance to water vapor is converted to conductance to CO_2 (g_{CO_2}) by adjusting for their diffusivities in air. Net assimilation at each canopy and light level is then modeled as

$$A_{net\,i,l} = g_{CO_2\,i,l} \times C_a \times \left(1 - \frac{C_i}{C_{a_{i,l}}}\right), \qquad (1)$$

where $A_{net\,i,l}$ is net assimilation at canopy level i and light level l, $g_{CO_{2\,i,l}}$ is stomatal conductance to CO_2 at canopy level i and light level l, C_a is atmospheric CO_2 concentration and $\frac{C_i}{C_{a_{i,l}}}$ is the ratio of internal (stomatal) to atmospheric CO_2 concentration at canopy level i and light level l. Leaf/atmosphere CO_2 ratio at each position and light level was modeled as (Katul *et al.*, 2000):

$$\frac{C_i}{C_{a\,i,l}} = \frac{g_{CO_2\,i,l} + \frac{b}{C_a}}{a + g_{CO_2 i,l}}, \qquad (2)$$

where a is CE and b is the CO_2 compensation point (Γ*). Total net assimilation of the canopy (A_{nC}) is calculated as the leaf area weighted sum of the assimilation modeled for each canopy level i and light level l (Schäfer *et al.*, 2003). In addition, for evaluation in 2006, an understory submodel was created to estimate C uptake from *G. baccata*, the predominant shrub in the understory.

Meteorological data

To estimate driving variables for the 4C-A model, air temperature (T_{air}) and relative humidity (RH, HMP45C Vaisala Inc., Helsinki, Finland), net radiation (R_n, NRLite, Kipp and Zonen Inc., Delft, the Netherlands), photosynthetic photon flux density (PPFD, Li-190, Li-Cor Instruments Inc., Lincoln, NE, USA), precipitation (P, TE525, Texas Electronics Inc., TX, USA), soil moisture

($\Theta\,m^3\,m^{-3}$, CS616, Campbell Scientific Inc., Logan, UT, USA), soil temperature at 5 cm depth (T_{soil}, 107-L, Campbell Scientific Inc.), wind speed and direction (05013-5, RM Young Co., MI, USA) were measured from a 19 m weather tower every 10 s, and half hourly averages recorded in a datalogger (CR23X, Campbell Scientific Inc.). Vapor pressure deficit (VPD) of forest air was calculated using RH and T_{air}.

Biometric measurements

A measurement plot was delineated within the forest stand upstream and within the footprint of the eddy flux tower located at the center point of an 80 m radius, and 54° angle 'pie slice' that included the trees measured for sap flux (see Table 1). During the dormant season of each year, diameters at breast height (DBH, 1.3 m above ground) of all trees with DBH > 2.5 cm within the plot were measured. In the summer of 2006, increment cores of 12 trees were sampled from the three major oak species at the site to determine sapwood area. These cores were used to determine the relationship between DBH and sapwood area and bark thickness.

For *Q. coccinia*, *Q. alba*, and *P. rigida*, allometric relationships developed by Whittaker & Woodwell (1968) were used to determine above- and belowground (coarse root) standing biomass, production, and leaf surface area. Allometric relationships developed for *Q. alba* by Whittaker & Woodwell (1968) were used for *Q. prinus* and *Q. velutina* (Table 1). In order to verify that the regression equations by Whittaker & Woodwell (1968) were valid for this forest, we compared (a) measured height vs. tree height calculated from allometric equations for each species, and (b) compared measured vs. calculated leaf area. For LAI estimates, 10 wire mesh traps of 0.42 m^2 area were positioned within 100 m of the eddy covariance tower, and litter was collected monthly, when present. Although understory trees were captured in the traps, the overall water flux did not include their sapwood area but their leaf area. However, the overall reduction in the G_C would be rather small and was evaluated through sensitivity analyses.

Average diameter tree growth was approximately 1–2 mm yr^{-1}, thus growth dynamics throughout the season were not applied. The measured and calculated heights did not significantly differ ($P > 0.07$ in each species); however for *Q. alba*, the measured height was 2–3 m higher than the calculated values in large trees (> 12 m in height), either due to measurement error or due to uncertainty in allometric equations.

Sap-flux measurements and scaling to G_C

Sap flux was measured with Kucera-type sensors inserted into the north side of the tree (Model P4.2, EMS, Brno, CZ) in six mature individuals of *Q. prinus* (sapwood area per unit ground area: $A_S : A_G = 1.98\,cm^2\,m^{-2}$, ~ 40% of total sapwood area), five of *Q. velutina* ($1.27\,cm^2\,m^{-2}$, ~ 25% of the total), and seven of *Q. coccinia* ($0.67\,cm^2\,m^{-2}$, ~ 13% of the total), using the heat balance method by Cermak *et al*. (1973). Starting in August of 2006, an individual *P. rigida* ($0.82\,cm^2\,m^{-2}$, ~ 16% of $A_S : A_G$, and 8% of basal area per unit ground area) was also monitored. Kucera type sensors consisted of three heated and one nonheated sensor with an input of 0.5–2.4 W, depending on the flow of water through the trunk of the tree. The heat balance method integrates throughout the depth of the sensor insertion. The knives (sensors) were inserted approximately 2 cm into the sapwood covering the entire sapwood depth, thus eliminating the need to account for radial patterns (Phillips *et al*., 1996). Unlike Granier sensors, the Kucera system has no correction for cases where sapwood depth is < 2 cm, as the probe blades are inserted according to the depth of the sapwood (Clearwater *et al*., 1999). In addition, unlike the Granier sensor technique, the calibration follows a linear function (see instruction manual EMS), thus any error in the baseline placement translates proportionally, and is likely to be small (Oishi *et al*., 2008). Power input data were recorded every 30 s and 30 min averages were stored in the system datalogger, then converted to sap flux ($g_{H_2O}\,m^{-2}_{sapwood}\,s^{-1}$) using system software (MINI32 version 4.1.5.0) programmed according to the instruction manual (May 2003, EMS).

Sap flux was scaled to stand transpiration (E_C) by multiplying the mean sap flux for each species (n = 5–7) by $A_S : A_G$ of each tree species for the measurement plot. The average sap flux of all oak trees was used to calculate E_C for *Q. stellata* and *Q. alba* trees by multiplying with respective $A_S : A_G$. In order to derive transpiration per unit leaf area (E_L), E_C was divided by LAI of each species, respectively. Canopy conductance (G_C) was calculated using E_L divided by VPD [Eqn (3)] after correcting for unit conversion (Köstner *et al*., 1992). This approach is valid when, (1) the canopy is well coupled to the atmosphere, and (2) storage contribution to the overall sap flow is negligible or is corrected for by time lagging transpiration to the driving force (VPD, Granier & Lousteau, 1994). We assumed that the canopy was well-coupled to the atmosphere (as per McNaughton & Jarvis, 1983; Clark *et al*., 2009), because temperature at 2 m height near the bottom of the canopy averaged only 1–2 °C lower than above canopy temperature in the summer, reflecting well-mixed conditions. Thus, we also assumed that leaf vapor pressure deficit is approximated by air VPD. Hence, VPD was used for canopy conductance calculations. In order to determine the storage contribution, E_L was lag regressed with the

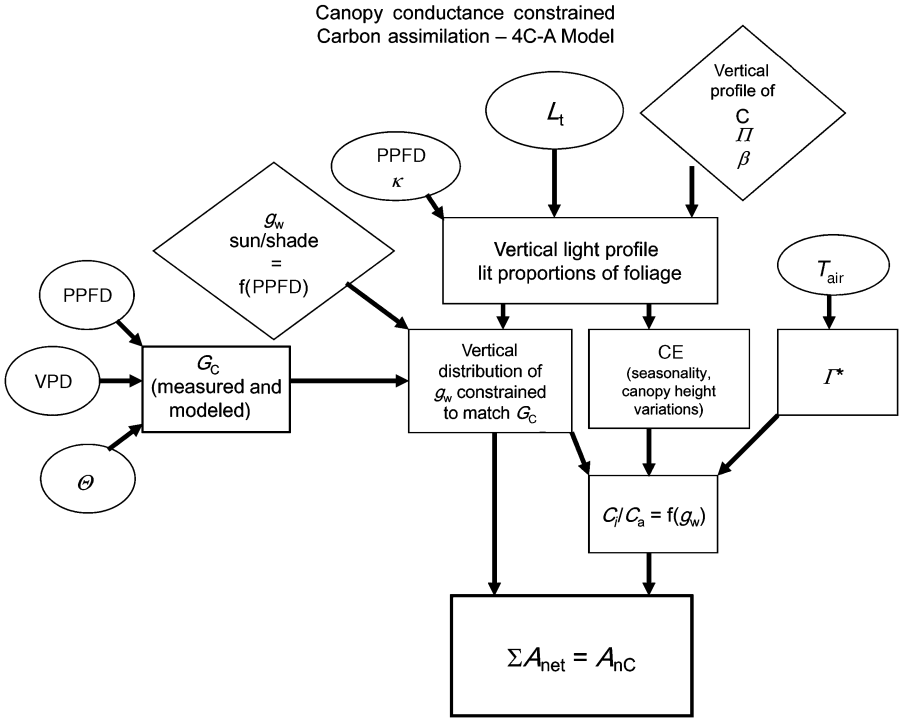

Fig. 1 Flowchart demonstrating input parameters and progression of the Canopy Conductance Constrained Carbon Assimilation (4C-A) model. Symbols, see text; ellipsoids, input variables; diamonds, derived parameters; rectangles, calculated variables; c, light transmission coefficient; π, clumping factor; β, silhouette to leaf area ratio; L_t, cumulative leaf area; κ, zenith angle

driving force VPD. The highest correlation coefficient was found at a lag time of 1 h ($r > 0.9$), thus, the storage contribution to the overall sap flow was corrected by a 1 h time lag of E_L to VPD (Granier & Lousteau, 1994).

Canopy conductance was calculated as (Köstner *et al.*, 1992)

$$G_C = \frac{G_V T_{air} \rho E_L}{VPD}, \quad (3)$$

where G_V (0.462 m^3 kPa kg^{-1} K^{-1}) is the universal gas constant adjusted for water vapor, T_{air} (in K) is air temperature, ρ is density of water in liquid form (998 kg m^{-3}), and E_L canopy transpiration per unit leaf area (mmol m^{-2} s^{-1}). Canopy conductance was only calculated for $\underline{VPD} > 0.6$ kPa in order to limit the error to a maximum of 10% (Ewers & Oren, 2000). For conditions of VPD < 0.6 kPa but PPFD > 0 and for gap filling, G_C was modeled with VPD and PPFD (see Fig. 1) after conducting a boundary line analysis (Schäfer *et al.*, 2000).

Physiological measurements and parameterization of 4C-A Canopy. All physiological measurements for parameterizing the model were made from May 7–September 30, 2006, to capture budbreak, the growing season, and onset of leaf fall. Parameterization required data on CE, CO_2 compensation point (Γ^*), and long-term internal to external CO_2 concentration ratio of the leaf, as estimated from stable carbon isotope ratios ($\delta^{13}C$). In addition, a generic light response curve of stomatal conductance to water vapor (g_w) is needed in order to calculate stomatal conductance at different canopy levels (Fig. 1).

The canopy was accessed using a 15 m scissor lift to measure leaf-level gas exchange with a LiCor 6400 portable photosynthesis system (LiCor Instruments Inc.). Response curves of A_{net} to internal CO_2 concentration (A_{net}–C_i) and g_w to light were generated. Leaf temperature and humidity within the chamber were also recorded. Measurements were made using leaves from five individuals each of *Q. prinus*, *Q. velutina*, and *Q. coccinia* at upper, mid- and lower canopy levels. Exact height of measurement was measured and recorded with a laser inclinometer (Haglöf, Sweden; VL400 Vertex Laser). Total number of leaves sampled per month were: $n = 3$ canopy levels × 3 species × 5 individuals = 45; over 5 months, a total of 225 gas exchange measurements were made. Measurements were made in trees growing adjacent to the sap-flux measurement plot (Table 1). In addition, concurrent gas exchange measurements of six *G. baccata*, three understory oaks, and three understory pine trees (*P. rigida*, each with diameter < 2.5 cm) were made. After each gas-exchange measurement was

completed, the leaf was harvested, leaf area and weight determined, dried at 80 °C for at least 48 h, and prepared for C, nitrogen (N) concentration, and ^{13}C and ^{15}N isotopic analyses. Samples were ground using a ball bearing mill and then encapsulated in tin capsules for mass spectrometer analysis at the Duke EnVironmental stable Isotope Laboratory (DEVIL) in Durham, NC, USA.

For the model, CE was calculated as the initial slope of the A_{net}–C_i curve. Values $>250\,\mu mol\,m^{-2}\,s^{-1}$ which represented the nonlinear portion were discarded, and linear regressions were performed on the remaining dataset (SAS version 9.1, Cary, NC, USA). A generic exponential response curve of PPFD to g_w with the best statistical fit for the data was used in the form:

$$g_w = c + a \times (1 - \exp^{(-b \times PPFD)}), \quad (4)$$

where a, b, and c are fitting parameters and g_w and PPFD as described above.

When g_w was fitted to PPFD using Eqn (4), large variations in the statistical fit were caused by early season values when leaves were not yet fully developed. Highest P values for this relationship were $P = 0.001$, and r^2 values ranged from 0.37 to 0.89.

Long-term internal to external CO_2 concentration ratio $\left(\frac{\overline{C_i}}{C_a}\right)$ of the leaf estimated from stable carbon isotope ratios ($\delta^{13}C$) were calculated as (Farquhar *et al*., 1989; Betson *et al*., 2007):

$$\frac{\overline{C_i}}{C_a} = \frac{\delta^{13}C_a - a - \delta^{13}C}{b - a}, \quad (5)$$

where $\frac{\bar{C}_i}{\bar{C}_a}$ is the long-term ratio of stomatal internal CO_2 concentration to atmospheric CO_2 concentration (overbar signifies averaging over time), $\delta^{13}C_a$ isotopic ratio of air, here measured during a period of minimal biotic activity (−12.9‰ during a cold period in January 2007), a is the discrimination of ^{13}C by air diffusion (−4.4‰), b is the fractionation during carboxylation (−27‰), and $\delta^{13}C$ is the isotopic ratio of the leaves where gas exchange was measured.

Understory. In order to estimate C uptake from the understory, a submodel was created from leaf gas-exchange measurements on the dominant understory shrub *G. baccata* in 2006 to assess its relative contribution to total forest C balance. Conductance of *G. baccata* was estimated over the course of the season with a multiple regression model of the form:

$$g_S = Y + A \times \log(VPD) + B \times \log(PPFD), \quad (6)$$

where A, B, and Y are regression parameters, VPD is vapor pressure deficit (in kPa), and PPFD is photosynthetic photon flux density for the understory that was modeled within the framework of 4C-A at the lowest canopy level (highest $P = 0.006$, $r^2 = 0.50$–0.83). Throughout the season conductance declined in 2006, partly because of increased drought and partly because the zenith angle declined, reducing incident radiation in the understory. Net assimilation of the *G. baccata* shrub layer was then modeled with 4C-A as above for the canopy.

Sensitivity analyses

CE and G_C were altered in order to assess the sensitivity of the model to these parameters. In addition, the canopy structure was simulated with a Gaussian profile. In order to simulate and asses an extension of the growing season as predicted under future climate conditions, the growing season in 2006 was prolonged by 1 week at the onset and 1 week at senescence of leaves. The 4C-A model was run as parameterized above, but with just one of these parameters varied to evaluate the impact on total annual C uptake. CE was modified (a) to reflect a constant CE (taking the mean of all CE calculated from measurements) throughout the canopy and season, (b) constant throughout the canopy but varied monthly, and (c) as in (a) but using the mean plus or minus one standard deviation (SD) of CE that was measured. Using the range of CE values measured (± 1 SD or 30%, mean CE = 0.06, SD = 0.02) will set the highest and lowest boundary of A_{nC} in this forest. Sensitivity analyses illustrated how much CE would need to be decreased by, i.e. through a second reflush, in order to affect A_{nC} appreciably.

Canopy conductance was varied by increasing or decreasing it by 20% of current, as may be expected through a stimulation through either leaf area losses (Pataki *et al*., 1998), or a decline that might be expected by elevated atmospheric CO_2 condition (Medlyn *et al*., 2001).

4C-Amodel evaluation

Model predictions were evaluated against (a) eddy covariance measurements of net ecosystem exchange (NEE) augmented with ecosystem respiration (R_{eco}, Clark *et al*., 2009), and (b) gross primary production (GPP) modeled from aboveground biomass estimates according to a relationship derived by Litton *et al*. (2007) at an annual time scale.

Eddy covariance measurements. On the centroid of the measurement plot, a 19 m tall tower was used to measure eddy fluxes and meteorological data. Fluxes of CO_2, H_2O, and energy were measured with a 3-dimensional sonic anemometer (RM 80001V, RM Young Co.), a closed-path infrared gas analyzer (LI-7000, Li-Cor Instruments Inc.), and a laptop PC. Details of the eddy covariance measurements are presented in

Published 2009

Clark *et al*. (2009). All meteorological and eddy flux data are available on the Ameriflux web site http://ornl.public.gov/ameriflux.

Net primary production (NPP). NPP was calculated as the difference between current and previous year standing biomass and annual litterfall data. Understory productivity was estimated using clip plots sampled at the time of peak biomass, and samples were sorted into foliage, stems, and other components, dried an weighed. In 2007, gypsy moth frass and leaf fragments in litterfall were collected biweekly, and added to litterfall totals to account for leaf mass lost due to herbivory. Aboveground NPP was used to estimate GPP according to Litton *et al*. (2007).

Canopy leaf area profile was measured using an upward-looking Light Detection and Ranging sensor (LiDAR) (N. Skowronski, unpublished results, Harding *et al*., 2001; Skowronski *et al*., 2007). This leaf area profile was remeasured periodically during the 2007 initial leaf-up, during defoliation, and after expansion of the second flush of leaves, in order to capture the temporal dynamics of the canopy's leaf area profile through the disturbance event.

Results

Sap-flux measurements and scaling to G_C

Sap-flux measurement and tree size were not correlated within species ($P > 0.13$), thus to scale sap flux to the entire stand, the mean sap flux for each species was used to calculate E_C for each species separately. When cores were taken from 12 trees, sapwood was clearly differentiated from hardwood by wood color. A linear relationship between sapwood depth and DBH was found ($r^2 = 0.60$, $P < 0.001$, $n = 12$). No relationship was found for bark thickness, thus the average bark thickness for each species was applied to the respective trees (mean 0.44 cm). For trees < 2.5 cm diameter, bark thickness was assumed 0.4 cm, and the entire cross-section to be sapwood.

In order to scale to E_L and thus to G_C, LAI is needed. Total canopy LAI of the tree stand derived from litter fall was $3.65\,m^2\,m^{-2}$ in 2006. Understory LAI was $0.45\,m^2\,m^{-2}$ in 2006, as estimated from clip plots ($n = 10$–20 of $1.0\,m^2$ plots). Leaf surface estimates from allometric relationships (as above) and litter fall traps produced similar results; LAI was $3.65\,m^2\,m^{-2}$ for the former vs. $3.33\,m^2\,m^{-2}$ for the latter in 2006. These results confirm the applicability of the allometric equations from Whittaker & Woodwell (1968) in this stand.

Physiological measurements and parameterization of 4C-A

Leaf-level measurements of CE were significantly different between canopy positions ($P < 0.0001$) and sampling month ($P < 0.0001$) but not between species ($P = 0.25$, Table 2). Species values were pooled and a positive linear relationship of CE with canopy height was found throughout the sampling season (Fig. 2a). However, the intercept and the slope of this relationship varied through the season, with the slope increasing and the intercept decreasing through time ($r^2 = 0.95$ for both; $P < 0.0001$ for both; Fig. 2b). The intercept of the height to CE relationship in the canopy leaves was consistent with CE measured in small understory oaks ($n = 3$), indicating that CE of these understory oaks did not differ from CE measured in the lower canopy of larger individuals (ANOVA repeated-measures monthly, $P = 0.28$). In addition, CE was linearly related to the intercept of the relationship of A_{net}–C_i ($r^2 = 0.56$, $P < 0.0001$, data not shown) and to leaf temperature ($r^2 = 0.22$, $P < 0.0001$, data not shown). On average, leaf temperature as measured with the LiCOR 6400 was 2 °C above air temperature and the resulting average vapor pressure difference between air and leaf was 0.09 kPa.

Maximum conductance to water vapor (g_{wmax}) measured with the LiCOR 6400 under light saturating condi-

Table 2 ANOVA (SAS PROC MIXED, v 9.1) *F*-values with indices for *P*-values of leaf physiological characteristics such as specific leaf area (SLA in $g\,cm^{-2}$), total % carbon (C) and % nitrogen (N) of dried green leaves, their $\delta^{13}C$ and $\delta^{15}N$, carboxylation efficiency (CE), photosynthetic CO_2 compensation point (Γ^*), internal to external CO_2 concentration ratio as derived from δC^{13} and maximum conductance to water vapor (g_{wmax}) for PPFD $> 1000\,\mu mol\,m^{-2}\,s^{-1}\,s^{-1}$ with respect to species (*Quercus prinus*, *Quercus velutina*, *Quercus coccinia*), month (May through September 2006) and canopy height (measured in m)

	SLA	%C	%N	$\delta^{13}C$	$\delta^{15}N$	CE	Γ^*	C_i/C_a ($\delta^{13}C$)	g_{wmax}
Species	3.24*	1.80	8.78***	1.38	5.04**	1.38	0.08	1.30	3.34*
Month	56.01***	20.70***	21.60***	64.66***	4.73**	52.17***	9.16***	64.21***	38.19***
Height	9.38***	1.37	1.98**	9.11***	5.61***	5.76***	0.59	9.07***	0.82

*$P < 0.05$, **$P < 0.01$, and ***$P < 0.0001$.

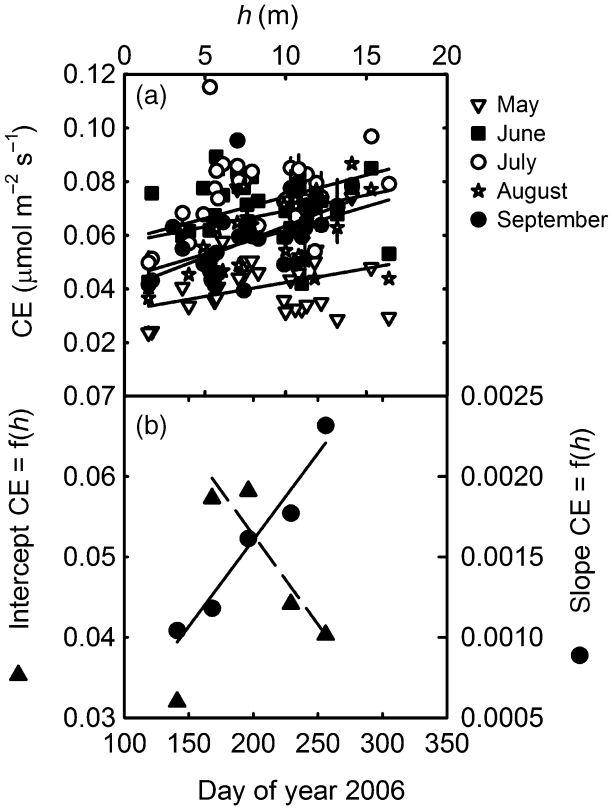

Fig. 2 (a) Relationship of carboxylation efficiency (CE) to canopy height (*h* in m) for each month separately. Intercept value for May was excluded in the relationship of the intercept vs. day of year in (b) derived from (a) relationship of the slope and the intercept of the relationship of CE to canopy height (*h*) as a function of day of year (DoY).

tions (PPFD $> 1000\,\mu mol\,m^{-2}\,s^{-1}$) was different for the three oak species ($P = 0.04$) and for each month ($P < 0.0001$). However, there was no difference in g_{wmax} for the different canopy levels ($P = 0.74$, Table 2). Thus, for PPFD-g_w functions, g_{wmax} was pooled over all canopy levels for each species and month. However, due to light attenuation in the canopy, leaves at the bottom had lower g_w than those in upper canopy positions. This pattern corresponded with lower specific leaf area (SLA $g\,cm^{-2}$) toward the bottom of the canopy (Table 2). Because g_{wmax} did not differ at different canopy levels, a clear distinction of shade and sun foliage was not expressed on a stomatal level in these oak species. The $\frac{C_i}{C_a}$ derived from $\delta^{13}C$ showed similar responses and statistics than $\delta^{13}C$ (Table 2). In this case, $\delta^{13}C$ showed significant differences between sampling periods and canopy height positions, but not among species (Table 2).

Leaf N-concentration remained at $\sim 1.8\%$–2.2% N dry weight throughout the growing season following spring leaf flush for canopy oak species, and then decreased significantly to only 45% of green leaf N content in litter (Fig. 3, black symbol). Leaf N decreased from top to bottom of the canopy, as did SLA and CE. Surprisingly, CE did not differ among species despite these differences in leaf N (Table 2, Fig. 3). In addition, there was no relationship between N and CE ($P = 0.27$), thus changes in N did not lead to changes in CE for this stand. For the understory species *G. baccata*, N dropped off significantly after late spring (open diamonds) and by September there was little measurable A_{net} activity. In the understory *P. rigida*, N concentration in the needles remained constant throughout the season, but by August, there was minute measurable A_{net} (Fig. 3). The $\delta^{15}N$ values were different between species, months and canopy height, suggesting differing sources of N among species, and/or different patterns of N reallocation among species (Table 2).

The total annual C uptake for the stand derived from the parameterized 4C-A for 2006 was $1244\,g\,C\,m^{-2}\,a^{-1}$. Canopy trees accounted for 98% of total A_{nC}, and the shrub layer contributed to the remainder. The same proportion is reflected in standing biomass, where the shrub layer comprises 2% of the total aboveground biomass (Table 1).

Published 2009

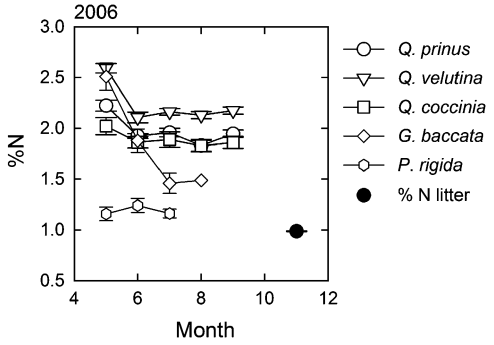

Fig. 3 Monthly mean nitrogen (N) concentration of leaves harvested following gas exchange measurements for each oak species and understory *Gaylussaccia baccata* and *Pinus rigida* (white symbols) and leaf litter for all oaks combined (black symbol) at the Rutgers University Pineland Research Station. Values are averaged throughout the canopy for representation purposes with errors representing one standard error of the mean (see Table 2).

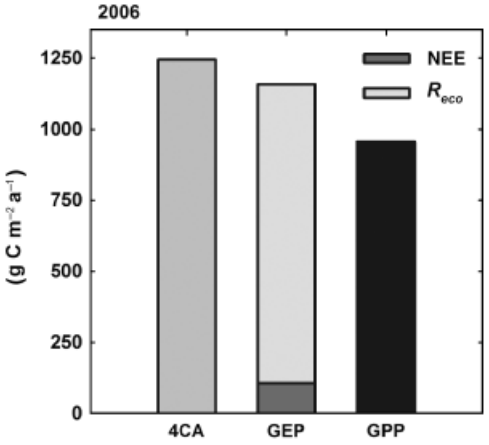

Fig. 4 Comparison of annual canopy net assimilation (A_{nC} in $g\,C\,m^{-2}\,a^{-1}$) modeled with the 4C-A model, gross ecosystem productivity (GEP) comprised of net ecosystem exchange (NEE) augmented with ecosystem respiration R_{eco} (both in $g\,C\,m^{-2}\,a^{-1}$) measured and modeled via the eddy covariance technique and gross primary productivity (GPP) modeled after Litton *et al.* (2007) (in $g\,C\,m^{-2}\,a^{-1}$) at the Rutgers University Pineland Research Station.

Sensitivity analyses

Using the mean CE throughout the canopy resulted in an 8% decrease in A_{nC} for the same year as compared with the original model. One standard deviation of the mean CE ($\pm$ 30%) changed A_{nC} + 2% and $-$21%, respectively. Varying CE by month and using the average CE applied throughout the canopy resulted in an 8% increase in A_{nC}, over mean values used in the model, and reflected differences in CE throughout the canopy and throughout the season affecting overall C uptake.

A $\pm$ 20% change in G_C resulted in overall annual C uptake of + 10% and $-$11% in A_{nC}, respectively. This result reflects interplay of parameters as predicted in Eqn (1): a proportional change in A_{nC} with a change in G_C. A partial compensation of reduced G_C is created through lower $\frac{C_i}{C_a}$ [see Eqn (2)] because of the interaction between $g_{CO_{2\,i,l}}$ and effective CE at each canopy level.

A Gaussian leaf area density profile resulted in an A_{nC} estimate of within 1% to the actual leaf area distribution. In an additional model run, the growing season was extended by a week at leaf out and a week at senescence. This resulted in an additional 100 $g\,C\,m^{-2}\,a^{-1}$ taken up by the canopy in 2006 which would help to partially compensate for C loss through disturbance.

4C-A model evaluation

Annual net carbon exchange (NEE) based on eddy-covariance measurements was $-105\,g\,C\,m^{-2}\,a^{-1}$, and annual ecosystem respiration (R_{eco}) was estimated to be 1051 $g\,C\,m^{-2}\,a^{-1}$ in 2006 (Clark *et al.*, 2009, Fig. 4). Gross ecosystem productivity (GEP = NEE + R_{eco}) was estimated at 1156 $g\,C\,m^{-2}\,a^{-1}$. Thus, A_{nC} modeled was 8% higher in 2006 than GEP estimated from flux measurements for 2006 at this stand.

Annual NPP in 2006 was 250 $g\,C\,m^{-2}\,a^{-1}$. GPP, estimated using a relationship derived by Litton *et al.* (2007), was 955 $g\,C\,m^{-2}\,a^{-1}$ (see Fig. 4). Overall, all estimates produce similar results in a range from 10% to 20% difference from each other.

Modeling A_{nC} *before and during gypsy moth defoliation*

Relative sap flux is shown in Fig. 5a for the entire canopy in 2005 (solid line) and 2006 (dotted line), and Fig. 5b for each species separately in 2007. In 2005 and 2006, peak sap flux occurred early in the growing season compared with distinctly lower sap fluxes at the same time in 2007 during defoliation (compare Fig. 5a and b). Although *Lymantria dispar* primarily feeds on oak, the data also showed marked decrease in sap flux in *P. rigida* (Fig. 5b, full circles) because *L. dispar* also defoliated *Pinus* tress and understory shrubs (and ate the plastic flagging of the branches that gas exchange was measured on).

Q. velutina sap flux had a slower postdefoliation recovery than the other oak species (Fig. 5b, full triangles). It is interesting to note, that the maximum sap flux occurred late in the season in 2007 compared with the previous years. Leaf area dynamics have been measured on a canopy basis by upward facing LiDAR; thus individual tree or species leaf area dynamics are not available. This affects G_C estimates, as some

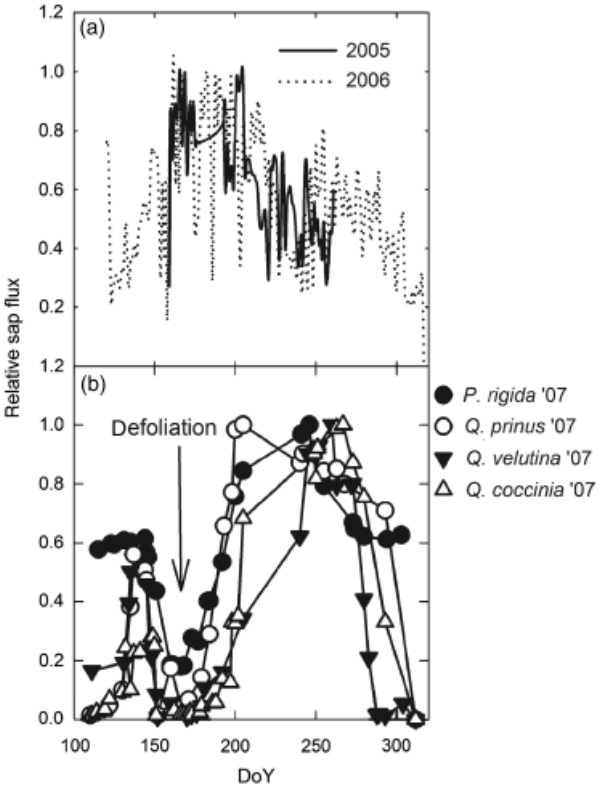

Fig. 5 (a) Relative sap flux to maximum combined for the entire canopy for 2005 (solid line) and 2006 (dotted line) and (b) for each species individually in 2007 (solid line with symbols: full circle *Pinus rigida*, open circle *Quercus prinus*, full triangle *Quercus velutina*, and open triangle *Quercus coccinia*) at the Rutgers University Pineland Research Station.

individuals or species may have reflushed at a later time point then others, thus G_C is either over or underestimated for that period.

Highest C uptake occurred in early summer, after the leaves have matured in 2005, concurrent with highest PPFD levels (Fig. 6a), similar to the pattern observed in 2006 (Fig. 6b). Because the shrub layer comprised a relatively small fraction of the total carbon budget, it was not considered in 2005 predefoliation and 2007 defoliation model runs. The prolonged late-season dry spell in 2006 did not affect A_{nC} to the extent of the 2007 defoliation (Fig. 6b). An overall leaf area decline from $4.2\,m^2\,m^{-2}$ in 2005 to $3.6\,m^2\,m^{-2}$ in 2006 was reflected with a proportional decline in A_{nC} over these years (Fig. 6b).

Gypsy moth defoliation in 2007 resulted in a strong decrease in early season A_{nC}, a period typically associated with peak levels of C uptake in this forest (Fig. 6b). During approximately 15% of the mature, 2007 leaf season for these deciduous trees at this site, a total defoliation was observed. Interestingly, there was a corresponding 25% reduction in A_{nC} in 2007 compared with the previous year. Timing and severity of impact is crucial for overall uptake capacity of the trees in this stand (Fig. 6b). In the latter part of the season, A_{nC} recovered to similar values as in the previous years (Fig. 6b) despite greatly reduced leaf area, suggesting compensation through higher G_C.

A summary of flux components, biomass estimates, and A_{nC} for all 3 years of investigation are displayed in Fig. 7. A_{nC} declined proportional to the decline in leaf area from 2005 to 2007. GPP also declined, but not to the same extent as A_{nC}. The proportion of C allocated to woody biomass decreased from 50% to 40% and leaf mass increased from 50% to 60% over the study period, respectively (Fig. 7, bars). GEP was similar in 2005 and 2006, but declined sharply in response to defoliation in 2007 (Fig. 7).

Discussion

Sap-flux measurements and scaling to G_C

In order to scale to E_C and ultimately G_C, proper sapwood area estimation need to be determined. A linear relationship of diameter to sapwood area was also found for other ring-porous species in a mixed hardwood stand (Oishi *et al*., 2008). If individual species leaf area dynamics can be determined then sap flux scaled G_C can become a predictive tool for forest recruitment, and survival modeling.

Physiological measurements and parameterization of the 4C-A model

CE was optimized throughout the season and canopy (Fig. 2, Table 2; see Meir *et al*., 2002). Consequently, upper canopy leaves exposed to higher light levels had higher N content, and, with higher CE, contributed more to total annual C uptake (data not shown). There was approximately 55% retranslocation of N at the end of the growing season (Fig. 3), supporting findings that nutrient cycling in the New Jersey Pine Barren forests is under tight plant control via internal recycling of N (Dighton *et al*., 2004). Indeed, the species-specific $\delta^{15}N$ in foliage collected in 2006 indicates there are differences between these species in their nitrogen supply dynamics, either internally through retranslocation or externally through different sources of N (Pardo *et al*., 2007). However, concurrent seasonal sampling of soil ^{15}N is needed to fully elucidate the mechanisms driving these differences (Evans & Belnap, 1999). Regardless of this and differences in total leaf N, seasonal CE was remarkably consistent between the three oak species (Fig. 2, Table 2), which may also explain the lack of

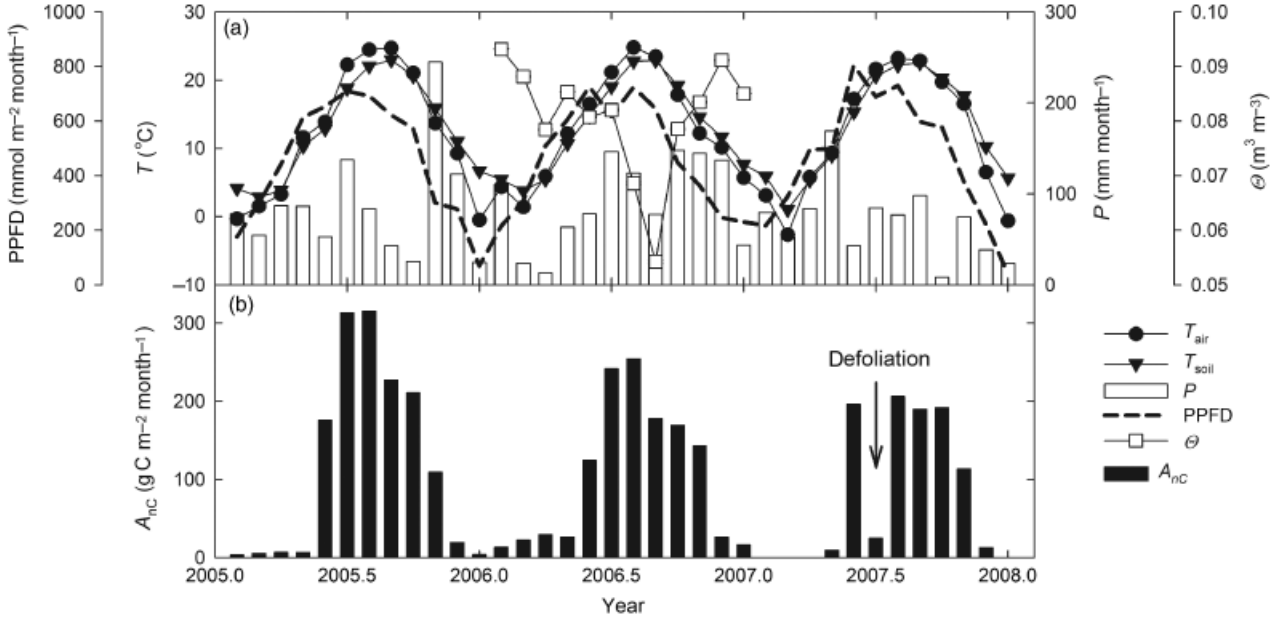

Fig. 6 (a) Monthly mean air temperature (black circles), soil temperature (black triangles, T in °C), volumetric soil moisture (open squares, Θ in $m^3\,m^{-3}$), monthly sum of precipitation (bars, P in mm), and photosynthetic photon flux density (dashed line, PPFD in $mol\,m^{-2}\,month^{-1}$) and (b) monthly sum of canopy assimilation modeled with 4C-A (A_{nC} in $g\,C\,m^{-2}\,month^{-1}$) for 2005–2007 at the Rutgers University Pineland Research Station.

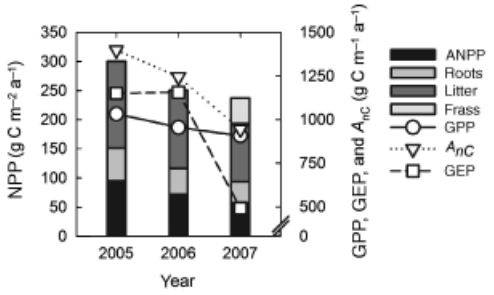

Fig. 7 Net primary production (bars, NPP in $g\,C\,m^{-2}\,a^{-1}$) derived from allometric equations and litter, gross primary production (circle, GPP in $g\,C\,m^{-2}\,a^{-1}$) derived from Litton *et al.* (2007), canopy net assimilation (triangles, A_{nC} in $g\,C\,m^{-2}\,a^{-1}$) modeled via 4C-A and gross ecosystem productivity (squares, GEP in $g\,C\,m^{-2}\,a^{-1}$) measured and modeled via the eddy covariance technique for 2005–2007 (Clark *et al.*, 2009) at the Rutgers University Pineland Research Station. Note: different y-axis for NPP and GPP, A_{nC} and GEP.

correlation between leaf N and CE in this stand. Similarly, a weak relationship between leaf N and A_{net} was observed in oak saplings (Rodrigues-Calcerrada *et al.*, 2008) and in *Pinus desiflora* needles (Han *et al.*, 2008) suggesting N-allocation different from RubisCO and N-allocation being a function of leaf/needle age. Likewise, in a controlled N-amendment study, CE did not show a clear response to N (Nakaji *et al.*, 2001). Meir *et al.* (2002) showed mixed results with spruce showing a weak relationship and oak a strong relationship of N to CE. In our study, the lack of correlation may indicate another limitation rather than N, such as P, or a decoupling of N and CE (Han *et al.*, 2008; Rodrigues-Calcerrada *et al.*, 2008) in order to allow maximum C uptake with minimum N investment.

Sensitivity analysis

Sensitivity analysis showed that accounting for CE attenuation throughout the canopy is crucial for modeling total A_{nC} (Fig. 4). Varying CE by 1 SD (± 30% of the mean), resulted in a net change of +2% and −21% in A_{nC} respectively; showing greater sensitivity toward lower CE estimates. In this model, apparent $\frac{C_i}{C_a}$ is a function of CE below the critical conductance value (Katul *et al.*, 2000; Schäfer *et al.*, 2003) and the critical conductance in turn is a function of $\frac{C_i}{C_a}$ and CE. Therefore, at high CE, the critical conductance at which saturation occurs is reached faster and $\frac{C_i}{C_a}$ is reached at lower g_{CO_2} values. Through these interactions the 30% increase in CE only resulted in 2% gain in A_{nC}.

The sensitivity analyses for canopy conductance showed an overall change of 10% in A_{nC} for a 20% change in G_C. Thus, when G_C is reduced by 20% – all else being equal – a reduction of up to $140\,g\,C\,m^{-2}\,a^{-1}$ may occur in this forest (for 2005 estimates). Small changes in G_C may not be discernibly translated into changes in A_{nC} with the 4C-A model. Given the uncertainty involved in measuring and estimating G_C

(Ewers & Oren, 2000), the logistical and technical difficulties in getting consistent and precise leaf-level gas exchange estimations of CE in forest canopies (Barker & Pinard, 2001), and uncertainty in estimating canopy leaf distribution profiles (Takeda *et al*., 2008), the robustness displayed by the 4C-A model in this study shows potential as a valuable and powerful tool in determining C-sequestration dynamics in forest ecosystems.

In the absence of a better description or direct measurement of canopy leaf area profile, the Gaussian canopy profile resulted in C uptake estimates similar to those using LiDAR data. This is useful information, if this model is applied to stands were little or no information on stand structure is available. However, the model is highly sensitive to annual leaf area dynamics and total leaf area for G_C calculation and A_{nC} estimates, for example, when A_{nc} for 2005 and 2006 are compared. Because of this sensitivity, seasonal leaf area dynamics have to be accounted for and measured as accurately as possible (see, e.g., Fig. 6b).

4C-A model evaluation

Predicted C uptake by 4C-A, compared favorably with eddy flux-derived estimates of GEP in 2006. We note that GEP calculated from flux measurements can vary by up to 11% with the gap filling method used (e.g. Clark *et al*., 2009). Similar results were obtained in a pine plantation in the North Carolina Piedmont, where flux components were 13% lower than A_{nC} estimated with 4C-A (Schäfer *et al*., 2003). Thus, estimates of C uptake predicted using the 4C-A model, are reasonable.

Biomass accumulation was accounted for by using allometric relationships (Whittaker & Woodwell, 1968) that estimated aboveground biomass and coarse roots, and augmented with litterfall. Using the relationship in Litton *et al*. (2007), GPP was estimated through aboveground biomass. However, 4C-A estimates net assimilation, which results in higher C estimates as biomass estimates alone. Biomass estimates fail to account for fine root growth, which can account between 300 and $700\,g\,C\,m^{-2}\,a^{-1}$ (Hamilton *et al*., 2002; Metcalfe *et al*., 2008). Also, biomass accounting does not include rhizodeposition (Hütsch *et al*., 2002; Phillips *et al*., 2008), or the production of dissolved organic carbon and volatile carbon components, thus GPP estimated in this manner may be underestimated.

Modeling A_{nC} before and during gypsy moth defoliation

When the 4C-A model was applied to the disturbance-free year of 2005, high leaf area and high G_C resulted in high A_{nC} estimates (Figs 6b and 7). During the extreme 2007 defoliation event, little C uptake occurred during the typical seasonal peak in carbon uptake (see arrow Fig. 6b). Total C uptake losses may have been partially compensated for by higher light availability at the onset of defoliation, and during the second leaf flush following complete defoliation as only 50% of the foliage re-emerged. At lower canopy levels, more foliage likely received direct beam radiation, thus a greater efficiency of C uptake per unit leaf occurs (Brodersen *et al*., 2008). Assuming equally proportional leaf area reduction, at each canopy level, higher radiation load in lower parts of the canopy may cause higher VPD at these levels, which could induce stomatal closure, countering potential C uptake at receiving higher light levels (Brodersen *et al*., 2008). Closure of G_C under high radiation was observed for the latter part of the season in 2007 (data not shown), and may have limited C uptake following defoliation. However, this canopy is tightly coupled to the atmosphere; therefore, a change in VPD at lower levels of the canopy is unlikely. This was verified as G_C response to VPD was not different between pre- and postdefoliation (see 'Material and methods,' Oren *et al*., 1999). A similar result was found in *Populus tremuloides* where G_C responded to VPD in a manner consistent with hydraulic consideration pre- and postdefoliation (Ewers *et al*., 2007).

Despite a large drop of leaf N in the second leaf flush (up to 60%, D. M. Gray, unpublished results) no changes in CE were incorporated in the model due to the lack of correlation between CE and leaf *N* (see 'Results'). The resulting A_{nC} estimates were comparable in the latter part of the season in 2007 to the previous years due to compensation through higher G_C (Fig. 6b). Pataki *et al*. (1998) demonstrated sap flux was not affected until 55% of leaf area was reduced in a controlled experiment. An appreciable effect on overall H_2O loss and CO_2 uptake can be expected only after major leaf area losses, as was also seen in this stand (Fig. 5b). Cunningham *et al*. (2009) showed a reduction in sap velocity of 25%–50% due to a 38% leaf necrosis by psyllids. However, the trees studied by Cunningham *et al*. (2009) were already suffering from a previous year's outbreak and may have been weakened at the time of study. In addition, when adjusted for functional leaf area, assuming comparable environmental conditions between the control and outbreak trees may have resulted in similar G_C values between treatments in their study (Cunningham *et al*., 2009).

With predicted shifts in climate (IPCC, 2007), an extended growing season may ensue in the temperate zone (Sitch *et al*., 2008) that would allow deciduous forests to take up more C. In our study forest, extended growing season would allow additional uptake of about $100\,g\,C\,m^{-2}\,a^{-1}$ under conditions similar to 2006, which would have compensated for one third of the losses

Published 2009

following *L. dispar* infestation and defoliation in 2007. Thus, the interactive effect of a prolonged season and insect outbreak frequency and severity could partially offset each other under some future climate scenarios. This forest had taken up $300\,g\,C\,m^{-2}\,a^{-1}$ less in 2007, thus of the 21% of upland forest this results in a total uptake loss of 0.020 Mt C for that year. This is a significantly less extensive event in space and severity than recently reported by pine bark beetles in Canada (Kurz *et al*., 2008). In addition, *L. dispar* does not directly kill most trees; therefore, resilience and recovery are possible. Whether resilience may be impacted by prolonged droughts or higher temperature in the future is not clear, but alteration of species composition is likely (Sitch *et al*., 2008).

As stated in the SOCCR report (CCSP, 2007), improved C-pool and flux inventories are needed for devising management practices to enhance C-sink strength in US forests. Improved models and establishing linkages between satellite derived imagery and C uptake strength will help garner more definite accounting strategies for carbon credit markets and mitigation practices. The 4C-A model is 'bridging the gap' by assessing C uptake strength for different species of this northeastern US oak/pine forest under disturbed and nondisturbed conditions. Further research to the linkage of satellite derived surface conductance to G_C in conjunction with satellite derived enhanced or normalized difference vegetation index would make the 4C-A model applicable to a wider range of sites and areas beyond the one investigated, and provide a powerful tool to assess changes in C uptake strength.

Conclusion

This study shows the 4C-A model estimated A_{nC} to within 15% of values using eddy-covariance and measured by forest census data in a nutrient-poor, mixed oak/pine forest. In order for 4C-A to perform adequately, G_C must be provided to within 20% of measured values, of CE seasonally averaged throughout the entire canopy profile, and utilize a Gaussian leaf density distribution to adequately reflect canopy structure. If the seasonal course of A_{nC} is to be modeled with adequate precision, CE must be measured at regular intervals and at discrete canopy increments throughout the season.

On a total ecosystem scale, this forest became a C-source in 2007 due to higher respiration rates not compensated for by C uptake throughout the growing season (Fig. 7; Clark *et al*., 2009). Generally, C-sink estimates for the United States may have been overestimated (Pacala *et al*., 2001), and the overall forest C-sink activity has declined since 1952 (CCSP, 2007). The report, and the research reported here, confirms that estimates need to take into account seasonal disturbance effects on leaf area and thus C uptake strength, and not solely stand biomass.

Acknowledgements

The authors express appreciation to the anonymous reviewers that greatly improved this manuscript. The authors would like to thank M. Xu for providing soil moisture data for 2006 and B. Langford, D. Miretskiy, and K. Paraiso for preparing leaf samples for C and N analysis. This project was funded in part from the National Science Foundation Grant Award #0456241 to E. P. H.

References

Baldocchi D, Meyers T (1998) On using micrometeorological and biophysical theory to evaluate carbon dioxide, water vapor and trace gas fluxes over vegetation: a perspective. *Agricultural and Forest Meteorology*, **90**, 1–25.

Barker MG, Pinard MA (2001) Forest canopy research: sampling problems, and some solutions. *Plant Ecology*, **153**, 23–28.

Betson NR, Johannisson C, Löfvenius MO, Grip H, Granström A, Högberg P (2007) Variation in the δ13C of foliage of *Pinus sylvestris* L. in relation to climate and additions of nitrogen: analysis of a 32-year chronology. *Global Change Biology*, **13**, 2317–2328.

Brodersen CR, Vogelmann TC, Williams WE, Gorton HL (2008) A new paradigm shift in leaf-level photosynthesis: direct and diffuse light are not equal. *Plant, Cell and Environment*, **31**, 159–164.

Campbell GS, Norman JM (1998) *An Introduction to Environmental Biophysics*, 2nd edn. Springer-Verlag, New York.

CCSP (2007) The First State of the Carbon Cycle Report (SOCCR): the North American Carbon Budget and Implications for the Global Carbon Cycle. In: *A Report by the US Climate Change Science Program and the Subcommittee on Global Change Research* (ed. King AW, Dilling L, Zimmerman GP, Fairman DM, Houghton RA, Marland G, Rose AZ, Wilbanks TJ) pp. 1–242. National Oceanic and Atmospheric Administration, National Climatic Data Center, Asheville, NC, USA.

Cermak J, Deml M, Penka M (1973) A new method of sap flow rate determination in trees. *Biologica Planetarium*, **15**, 171–178.

Chambers JQ, Fisher JI, Zeng H, Chapman EL, Baker DB, Hurtt GC (2007) Hurricane Katrina's Carbon Footprint on US Gulf Coast Forests. *Science*, **318**, 1107.

Clark KL, Skowronski N, Hom J (2009) Invasive insects impact forest carbon dynamics. *Global Change Biology*, doi: 10.1111/j.1365-2486.2009.01983x.

Clearwater MJ, Meinzer FC, Andrade JL, Goldstein G, Holbrook NM (1999) Potential errors in measurement of nonuniform sap flow using heat dissipation probes. *Tree Physiology*, **19**, 681–687.

Collatz GJ, Ball JT, Griver C, Berry JA (1991) Physiological and environmental regulation of stomatal conductance, photosynthesis and transpiration: a model that includes a laminar boundary layer. *Agricultural and Forest Meteorology*, **54**, 107–136.

Cunningham SA, Pullen KR, Colloff MJ (2009) Whole-tree sap flow is substantially diminished by leaf herbivory. *Oecologia*, **158**, 633–640.

Dale VH, Joyce LA, McNulty S *et al*. (2001) Climate change and forest disturbance. *BioScience*, **51**, 723–734.

DePury DGG, Farqhar GD (1997) Simple scaling of photosynthesis from leaves to canopies without the error of big leaf models. *Plant, Cell and Environment*, **20**, 537–557.

Dighton J, Tuininga AR, Gray DM, Huskins RE, Belton T (2004) Impacts of atmospheric deposition on New Jersey pine barrens forest soils and communities of ectomycorrhizae. *Forest Ecology and Management*, **201**, 131–144.

Eisenbies MH, Davidson C, Johnson J, Amateis R, Gottschalk K (2007) Tree mortality in mixed pine-hardwood stands defoliated by the European gypsy moth (*Lymantria dispar* L.). *Forest Science*, **53**, 683–691.

Evans RD, Belnap J (1999) Long-term consequences of disturbance on nitrogen dynamics in an arid ecosystem. *Ecology*, **80**, 150–160.

Ewers BE, Mackay DS, Samanta S (2007) Interannual consistency in canopy stomatal conductance control of leaf water potential across seven tree species. *Tree Physiology*, **27**, 11–24.

Ewers BE, Oren R (2000) Analysis of assumptions and errors in the calculation of stomatal conductance from sap-flow measurements. *Tree Physiology*, **20**, 579–589.

Fajvan MA, Rentch J, Gottschalk K (2008) The effects of thinning and gypsy moth defoliation on wood volume growth in oaks. *Trees*, **22**, 257–268.

Farquhar GD, Ehleringer JR, Hubick KT (1989) Carbon isotope discrimination and photosynthesis. *Annual Review of Plant Physiology and Plant Molecular Biology*, **40**, 503–537.

Farquhar GD, von Caemmerer S, Berry JA (1980) A biochemical model of photosynthetic CO_2 assimilation in leaves of C3 species. *Planta*, **149**, 78–90.

Gough CM, Vogel CS, Harrold KH, George K, Curtis PS (2007) The legacy of harvest and fire on ecosystem carbon storage in a north temperate forest. *Global Change Biology*, **13**, 1935–1949.

Gough CM, Vogel CS, Schmid HP, Curtis PS (2008) Controls of annual forest carbon storage: lessons from the past and predictions for the future. *Bioscience*, **58**, 609–622.

Granier A, Lousteau D (1994) Measuring and modeling the transpiration of a maritime pine canopy from sap-flow data. *Agricultural and Forest Meteorology*, **71**, 61–81.

Gromtsev A (2002) Natural disturbance dynamics in the boreal forests of European Russia: a review. *Silva Fennica*, **36**, 41–55.

Hamilton JG, DeLucia EH, George K, Naidu SL, Finzi AC, Schlesinger WH (2002) Forest carbon balance under elevated CO_2. *Oecologia*, **131**, 250–260.

Han Q, Kawasaki T, Nakano T, Chiba Y (2008) Leaf-age effects on seasonal variability on photosynthetic parameters and its relationship with leaf mass per area and leaf nitrogen concentration within a *Pinus densiflora* crown. *Tree Physiology*, **28**, 551–558.

Harding DJ, Lefsky MA, Parker GG, Blair JB (2001) Laser altimeter canopy height profiles: methods and validation for closed-canopy, broadleaf forests. *Remote Sensing of Environment*, **76**, 283–297.

Hütsch BW, Augustin J, Merbach W (2002) Plant rhizodeposition – an important source for carbon turnover in soils. *Journal of Plant Nutrition and Soil Science*, **165**, 397–407.

IPCC 2007 Summary for Policymakers. In: *Climate Change 2007: The Physical Science Basis. Contribution of Working Group I to the Fourth Assessment Report of the Intergovernmental Panel on Climate Change* (eds Solomon S, Qin D, Manning M, Chen Z, Marquis M, Averyt KB, Tignor M, Miller HL), pp. 1–21. Cambridge University Press, Cambridge, UK.

Jönsson AM, Appelberg G, Harding S, Bärring L (2008) Spatio-temporal impact of climate change in the activity and voltinism of the spruce bark beetle, *Ips typographus*. *Global Change Biology*, **15**, 486–499.

Katul GG, Ellsworth DS, Lai C-T (2000) Modeling assimilation and intercellular CO_2 from measured conductance: a synthesis of approaches. *Plant, Cell and Environment*, **23**, 1313–1328.

Kim H-S, Oren R, Hinckley TM (2008) Actual and potential transpiration and carbon assimilation in an irrigated poplar plantation. *Tree Physiology*, **28**, 559–577.

Köstner BMM, Schulze E-D, Kelliher FM *et al*. (1992) Transpiration and canopy conductance in a pristine broad-leaved forest of *Nothofagus*: an analysis of xylem sap flow and eddy correlation measurements. *Oecologia*, **91**, 350–359.

Kurz WA, Dymond CC, Stinson G *et al*. (2008) Mountain pine beetle and forest carbon feedback to climate change. *Nature*, **452**, 987–990.

Lai C-T, Katul GG, Oren R, Ellsworth DE, Schäfer KVR (2000) Modeling CO_2 and water vapor turbulent flux distributions within a forest canopy. *Journal of Geophysical Research*, **105**, 26333–26351.

Landsberg JJ, Waring RH (1997) A generalized model of forest productivity using simplified concepts of radiation-use efficiency, carbon balance, and partitioning. *Forest Ecology and Management*, **95**, 209–228.

Leuning R (1995) A critical appraisal of a combined stomatal-photosynthesis model for C_3 plants. *Plant, Cell and Environment*, **18**, 339–355.

Little S (1998) Fire and plant succession in the New Jersey Pine Barrens. In: *Pine Barrens: Ecosystem and Landscape* (ed. Forman RTT), pp. 297–314. Rutgers University Press, New Brunswick, NJ.

Litton CM, Raich JW, Ryan MG (2007) Carbon allocation in forest ecosystems. *Global Change Biology*, **13**, 2089–2109.

Markley ML (1998) Soil series in the Pine Barrens. In: *Pine Barrens: Ecosystem and Landscape* (ed. Forman RTT), pp. 81–93. Rutgers University Press, New Brunswick, NJ.

Matlack GR, Gleeson SK, Good RE (1993) Treefall in a mixed oak-pine coastal plain forest: immediate and historical causation. *Ecology*, **74**, 1559–1566.

McCarthy HR, Oren R, Finzi AF, Ellsworth DS, Kim H-S, Johnson KH, Millar B (2007) Temporal dynamics and spatial variability in the enhancement of canopy leaf area under elevated atmospheric CO_2. *Global Change Biology*, **13**, 2479–2497.

McCarthy HR, Oren R, Kim H-S, Johnson KH, Maier C, Pritchard SG, Davis MA (2006) Interaction of ice storms and management practices on current carbon sequestration in forests with potential mitigation under future CO_2 atmosphere. *Journal of Geophysical Research*, **111**, D15103, doi: 10.1029/2005JD006428.

McNaughton KG, Jarvis PG (1983) Predicting effects of vegetation changes on transpiration and evaporation. In: *Water Deficits and Plant Growth*, Vol. VII (ed Kozlowski TT), pp. 1–47. Academic Press, San Diego.

McNulty SG (2002) Hurricane impacts on US forest carbon sequestration. *Environmental Pollution*, **116**, S17–S24.

Medlyn BE, Barton CVM, Broadmeadow MSJ *et al*. (2001) Stomatal conductance of forest species after long-term exposure to elevated CO_2 concentration: a synthesis. *New Phytologist*, **149**, 247–264.

Meir P, Kruijt B, Broadmeadow M *et al*. (2002) Acclimation of photosynthetic capacity to irradiance in tree canopies in relation to leaf nitrogen concentration and leaf mass per area. *Plant, Cell and Environment*, **25**, 343–357.

Metcalfe DB, Meir P, Aragao LEOC *et al*. (2008) The effects of water availability on root growth and morphology in an Amazon rainforest. *Plant Soil*, **311**, 189–199.

Nakaji T, Fukami M, Dokiya Y, Izuta T (2001) Effects of high nitrogen load on growth, photosynthesis and nutrient status of *Cryptomeria japonica* and *Pinus densiflora* seedlings. *Trees*, **15**, 453–461.

Oishi AC, Oren R, Stoy PC (2008) Estimating components of forest evapotranspiration: a footprint approach for scaling sap flux measurements. *Agricultural and Forest Meteorology*, **148**, 1719–1732.

Oren R, Sperry JS, Katul GG *et al*. (1999) Intra-and inter-specific responses of canopy stomatal conductance to vapour pressure deficit. *Plant, Cell and Environment*, **22**, 1515–1526.

Pacala SW, Hurtt GC, Baker D *et al*. (2001) Consistent land- and atmosphere-based US carbon sink estimates. *Science*, **292**, 2316–2320.

Pan Y, Birdsey R, Hom J, McCullough K, Clark K (2006) Improved estimates of net primary productivity from MODIS satellite data at regional and local scales. *Ecological Applications*, **16**, 125–132.

Pardo LH, McNulty SG, Boggs JL, Suke S (2007) Regional pattern in foliar ^{15}N across a gradient of nitrogen deposition in the northeastern US. *Environmental Pollution*, **149**, 293–302.

Pataki DE, Oren R, Phillips N (1998) Responses of sap flux and stomatal conductance of *Pinus taeda* L. trees to stepwise reduction in leaf area. *Journal of Experimental Botany*, **49**, 871–878.

Phillips NG, Oren R, Zimmermann R (1996) Radial patterns of xylem sap flow in non-, diffuse and ringporous tree species. *Plant, Cell and Environment*, **19**, 983–990.

Published 2009

Phillips RP, Erlitz Y, Bier R, Bernhardt ES (2008) New approach for capturing soluble root exudates in forest soils. *Functional Ecology*, **22**, 990–999.

Rhodehamel EC (1998) Geology of the Pine Barrens of New Jersey. In: *Pine Barrens: Ecosystem and Landscape* (ed. Forman RTT), pp. 39–60. Rutgers University Press, New Brunswick, NJ.

Rodrigues-Calcerrada J, Reich PB, Rosenqvist E, Pardos JA (2008) Leaf physiological versus morphological acclimation to high-light exposure at different stages of foliar development in oak. *Tree Physiology*, **28**, 761–771.

Roxburgh SH, Wood SW, Mackey BG, Woldendorp G, Gibbons P (2007) Assessing the carbon sequestration potential of managed forests: a case study from temperate Australia. *Ecological Application*, **43**, 1149–1159.

Running SW (2008) Ecosystem disturbance, carbon and climate. *Science*, **321**, 652–653.

Ryan KC (2002) Dynamic interactions between forest structure and fire behavior in boreal ecosystems. *Silva Fennica*, **36**, 13–39.

Schäfer KVR, Oren R, Ellsworth DS *et al*. (2003) Exposure to an enriched CO_2 atmosphere alters carbon assimilation and allocation in a pine forest ecosystem. *Global Change Biology*, **9**, 1378–1400.

Schäfer KVR, Oren R, Tenhunen JD (2000) The effect of tree height on crown level stomatal conductance. *Plant, Cell and Environment*, **23**, 365–375.

Scheller RM, van Tuyl S, Clark K, Hayden NG, Hom J, Mladenoff DJ (2008) Simulation of forest change in the New Jersey Pine Barrens under current and pre-colonial conditions. *Forest Ecology and Management*, **255**, 1489–1500.

Schulze E-D (2006) Biological control of the terrestrial carbon sink. *Biogeosciences*, **3**, 147–166.

Sitch S, Huntigford C, Gedney N *et al*. (2008) Evaluation of the terrestrial carbon cycle, future plant geography and climate-carbon cycle feedbacks using five Dynamic Global Vegetation Models (GDVMs). *Global Change Biology*, **14**, 2015–2039.

Skowronski N, Clark K, Nelson R, Hom J, Patterson M (2007) Remotely sensed measurements of forest structure and fuel loads in the Pinelands of New Jersey. *Remote Sensing of Environment*, **108**, 123–129.

Takeda T, Oguma H, Sano T, Yone Y, Fujinuma Y (2008) Estimating the plant area density of a Japanese larch (*Larix kaempferi* Sarg) plantation using ground-based laser scanner. *Agricultural and Forest Meteorology*, **148**, 428–438.

Thornton PE, Law BE, Gholz HL *et al*. (2002) Modeling and measuring the effect of disturbance history and climate on carbon and water budgets in evergreen needleleaf forests. *Agricultural and Forest Meteorology*, **113**, 185–222.

Vargas R, Allen MF, Allen EB (2008) Biomass and carbon accumulation in a fire chronosequence of a seasonally dry tropical forest. *Global Change Biology*, **14**, 109–124.

Wang YP, Jarvis PG (1990) Description and validation of an array model – MAESTRO. *Agricultural and Forest Meteorology*, **51**, 257–280.

Whittaker RH, Woodwell GM (1968) Dimension and production relations of Trees and shrubs in the Brookhaven Forest, New York. *The Journal of Ecology*, **56**, 1–25.

Published 2009
